Published online 22 March 2017

Nucleic Acids Research, 2017, Vol. 45, No. 10 ***5829–5837***
doi: 10.1093/nar/gkx203

Functional anatomy of the immunoglobulin heavy chain 3′ super-enhancer needs not only core enhancer elements but also their unique DNA context

Sandrine Le Noir[1,*], François Boyer[1], Sandrine Lecardeur[1], Mylène Brousse[1], Zeliha Oruc[1], Jeanne Cook-Moreau[1], Yves Denizot[1] and Michel Cogné[1,2,*]

[1]UMR 7276 CNRS and Université de Limoges: Contrôle de la Réponse Immune B et Lymphoprolifération, 2 rue du Dr. Descottes, 87025 Limoges, France and [2]Institut Universitaire de France, Paris, France

Received December 27, 2016; Revised March 14, 2017; Editorial Decision March 17, 2017; Accepted March 22, 2017

ABSTRACT

***Cis*-regulatory elements feature clustered sites for transcription factors, defining core enhancers and have inter-species homology. The mouse *IgH* 3′ regulatory region (*3'RR*), a major B-cell super-enhancer, consists of four of such core enhancers, scattered throughout more than 25 kb of packaging 'junk DNA', the sequence of which is not conserved but follows a unique palindromic architecture which is conserved in all mammalian species. The 3'RR promotes long-range interactions and potential IgH loops with upstream promoters, controlling class switch recombination (CSR) and somatic hypermutation (SHM). It was thus of interest to determine whether this functional architecture also involves the specific functional structure of the super-enhancer itself, potentially promoted by its symmetric DNA shell. Since many transgenic 3'RR models simply linked core enhancers without this shell, it was also important to compare such a 'core 3'RR' (c3'RR) with the intact full-length super-enhancer in an actual endogenous IgH context. Packaging DNA between 3'RR core enhancers proved in fact to be necessary for optimal SHM, CSR and IgH locus expression in plasma cells. This reveals that packaging DNA can matter in the functional anatomy of a super-enhancer, and that precise evaluation of such elements requires full consideration of their global architecture.**

INTRODUCTION

In mature B-cells, a major 3′ *cis*-regulatory super-enhancer controls accessibility of immunoglobulin heavy chain (IgH) constant (*C*) genes to transcription and to IgH changes initiated by activation-induced deaminase (AID) (1–3). In the mouse, this 3′regulatory region (*3'RR*) is made up of a cluster of four core enhancers: *hs3a, hs1,2*, *hs3b* and *hs4*. It barely influences *V(D)J* recombination in B-cell progenitors, except for paradoxically silencing early transcription in pro-B-cells, and barely affects basal pVH transcription in resting B-cells (4,5). By contrast in plasma cells, the 3'RR strongly contributes to increased IgH transcription which physiologically marks the plasma cell stage (6). The 3'RR is also the master *cis*-regulatory region controlling conventional class switch recombination (CSR), (7,8) locus suicide recombination (LSR) (9) and somatic hypermutation (SHM) (10) by modulating germline transcription of C genes in activated B-cells, chromatin remodeling of switch (S) regions, AID activity on targeted sequences, and also probably the synapsis between broken S regions which terminates CSR (1,11). In addition, to being bound by specific transcription factors, 3'RR core enhancers are transcribed into eRNA (9), and regulated in their function by a distantly transcribed long non-coding RNA (lncRNA CSR) (3).

In all mammalians studied, the upstream 3'RR enhancers are embedded within a long and uniquely palindromic DNA region, with the last enhancer (*hs4)* lying outside and downstream of this palindrome (1,12); for example in the mouse, the *hs3a*, *hs1,2* and *hs3b* core elements are found within a ∼25-kb dyad symmetry, with *hs1,2* at the center, flanked by inverted repeated intervening sequences (*IRIS*) and bound by inverted copies of the *hs3a/hs3b* enhancers (Figure 1A). In humans, the *3'RR* is duplicated and each 3'RR is composed of only three core enhancers (*hs3*, *hs1.2* and *hs4*) with *hs1,2* also flanked by *IRIS.* Despite the modest activity of each of the *3'RR* core enhancers *in vitro*, they altogether build a synergistic and potent super-enhancer notably efficient in transgenes, especially when a palindromic architecture is preserved (13). *IRIS* lack DNase1 hypersensitivity and obvious sites for transcription factors and are mostly made up of non-coding repetitive DNA. Some of these 'like switch' repeats resemble S regions and likely pro-

*To whom correspondence should be addressed. Tel: +33 519564200; Fax: +33 555435897; Email: cogne@unilim.fr
Correspondence may also be addressed to Dr. Sandrine Le Noir. Email: sandrine.le-noir@unilim.fr

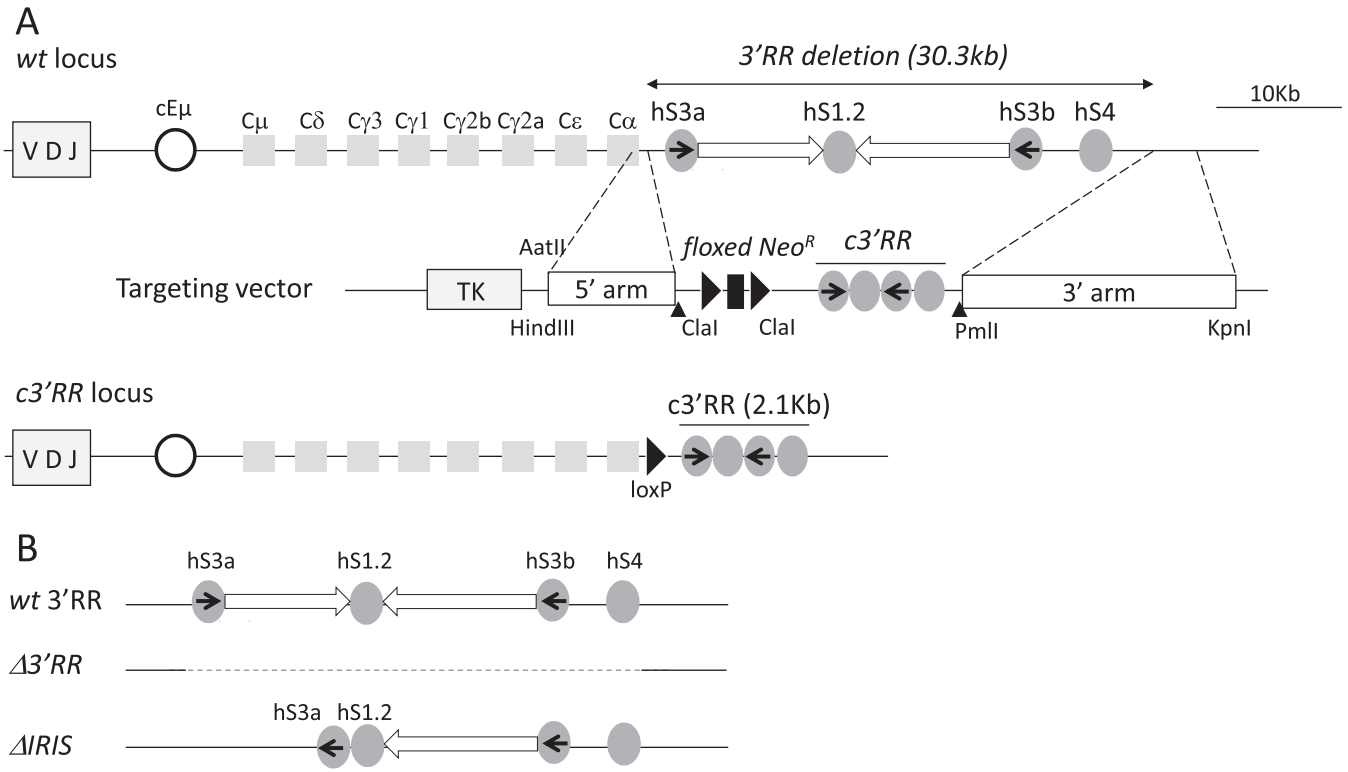

Figure 1. Genomic organization of the c3'RR locus and 3'RR mutant mice. (**A**) Murine *IgH* locus (not to scale); Ig gene segments are indicated; arrows represent the palindromic inverted repeats (*top*) (*complete sequence of the 3'RR is provided in* (12) *repetitive elements are further described in* (9)). Targeting vector; arrow heads represent CRISPR/cas 9 primers (*middle*). Successfully targeted *c3'RR* allele (*bottom*). (**B**) 3'RR mutant mice used in this study. The *Δ3'RR* deletion eliminates the four enhancers and the palindromic region. The *ΔIRIS* locus carries an inverted *hs3a* enhancer and lacks the intervening sequences between *hs3a* and *hs1,2.*

mote *IgH* deletion events during LSR (9). Although highly divergent in different species, *IRIS* sequences always stand as inverted copies on both sides of *hs1,2,* thus preserving 3'RR symmetry and strongly suggesting that their architectural role might be required for IgH expression. We recently deleted the upstream side of the palindrome (the 10 kb-long 5′ IRIS) in the endogenous locus in Δ*IRIS* knock-out mice where all 3'RR core enhancers were preserved and the downstream copy of the *IRIS* remained unaltered (14). This affected SHM and to a lesser extent CSR. It was, however, questionable whether this phenotype resulted from the loss of an unknown *cis*-acting sequence included in the 5'IRIS, from the decreased distance between *hs3a* and *hs1,2*, or from loss of the 3'RR symmetry. 3'RR activity is also often considered as simply the sum of all core enhancer activities, and combinations of all 3′ core enhancers are thus widely used as 3'RR models in transgenes (15–19). It has also recently been observed in the CH12 B-cell line, that replacement of the 28 kb-long 3'RR with a simple combination of all four core enhancers preserved or even increased *IgH* locus accessibility to *Cα* CSR (20). Since transgenes are susceptible to random insertion effects and since immortalized B-cell lines such as CH12 might be frozen with regards to chromatin marks and accessibility, we found it important to check the real effect of 3'RR replacement in the context of the endogenous *IgH* locus of primary B-cells. Compared with the recent *ΔIRIS* mouse lacking only the 5′ IRIS, the herein reported 'core 3'RR' (*c3'RR*) mouse model completely lacks 3'RR packaging DNA. Interestingly, this complete elimination of packaging DNA around core enhancers strongly affects the main activities of the 3'RR, notably with regards to IgH expression in plasma cells, SHM and class switching. It, however, appears very similar to the phenotype of ΔIRIS mice, and thus further indicates that the 3'RR IRIS are only active when present in two copies, with a role that differs from that of a core enhancer, and is solely architectural: providing the palindromic framework that ensures optimal function of 3'RR core enhancers.

MATERIALS AND METHODS

Mice

One hundred twenty-nine *wt* mice (from Charles River Laboratories, France) *Δ3'RR* and *c3'RR* mice (in a 129 background) were used. Our study was approved by the local ethics committee review board (Comité Régional d'Ethique sur l'Expérimentation Animale du Limousin, Limoges, France).

Vector construction and embryonic stem cell screening

The vector used for homologous recombination assembled a previously described 3′ homology arm (located 3.5 kb downstream of hs4) (8) followed by the thymidine kinase (*Tk*) gene, and a 5′ arm homologous to the region

upstream of *hs3a* (amplified using primers listed in Supplementary Table S1). A *floxed* neomycin resistance gene (neo^R) together with a synthetic 2.1 kb *c3'RR* cassette were inserted in between both arms, replacing the entire 3'RR. Two CRISPR vectors were created using the pX330 vector (Addgene, Cambridge, USA), for production of two guide RNAs able to target Cas9 recombinase at both ends of the desired 3'RR deletion. The various PCR primers and CRISPR sequences used are reported in Supplementary Table S1.

Cells of the embryonic stem (ES) cell line CK35 were transfected with 8μg of linearized targeting vector and 0.5 μg of each CRISPR/cas9 vector by electroporation and selected using 300 μg /ml geneticin and 2 μg/ml gancyclovir.

Immunization

For immunization experiments, groups of 8-week-old mice (>5 mice per genotype) were immunized by intraperitoneal injection of 200 μl SRBC and analyzed 8 after days.

Cell culture

Splenocytes were collected, red blood cells were lysed and cells were CD43-depleted using CD43 microbeads (Miltenyi Biotec). Spleen B lymphocytes were cultured for 5 days in RPMI containing 10% FCS with either LPS (20 μg/ml) + IL4 (40 ng/ml) (Peprotech), or LPS (20 μg/ml) + IFNγ (2 ng/ml) (RD systems) or LPS (20 μg/ml) + TGFβ (2 ng/ml) (RD systems). Supernatants were recovered at day 4 and stored at –20°C until used. Culture samples were harvested daily for RNA extraction.

CSR analysis

At day 4, *in vitro* activated splenic B-cells were incubated with anti-B220-BV510 (clone RA3-6B2, Biolegend), anti-IgG_1-PE (clone A85-1, BD Pharmingen), anti-IgG_3-FITC (clone R40-82, Beckton Dickinson) antibodies and analysed on a BD Pharmingen Fortessa LSR2 using BD FACSDiva software (BD Biosciences, San Jose, CA, USA).

ELISA

ELISAs for IgM, IgG_1, IgG_3, IgG_{2a}, IgG_{2b} and IgA were performed on sera and *in vitro* stimulated B-cell supernatants from *Δ3'RR*, *c3'RR* and *wt* mice, as previously described (8).

Real time quantitative PCR

Four day *in vitro* stimulated splenocytes (LPS + appropriate cytokines) were harvested and RNA was extracted to evaluate I_x-C_x germline transcripts (GLT). The kinetics of I_μ-C_x post switch transcription (PST) was followed daily. RNA and cDNA were prepared using standard techniques. Quantitative PCR was performed using SYBR® Green (Takara). PCR primers used for determination of I_x-C_x and $I\mu$-C_x transcripts are reported in Supplementary Table S1.

Flow cytometry and cell sorting

Cell suspensions from Peyer's patches were labeled with anti-B220-APC- (Clone RA3-6B2, Biolegend), GL7-PE-(BD) conjugated antibodies. Sorting of $B220^+/GL7^+$ cells was performed on a FACS ARIA 3 (BD Biosciences).

SHM analysis

SHM analysis was performed as described (10) in the J_H4 intron, *Jk5* intron and *Sμ* region from sorted B220+/GL7+ cells from Peyer's patches. PCR products (100 ng) were fragmented using the Ion Shear Plus Reagents kit (Life Technologies), then barcodes and adaptors were ligated using Ion Xpress Plus Fragment (Life Technologies). Fragments around 200 pb were selected using 2% E-Gel size select (Life Technologies) and sequenced on an Ion Proton™ System. Raw fastq files were generated using Ion Torrent Suite (adapter- and barcode-trimmed) and mapped to the reference sequences using BWA-MEM (Li, 2013). Aligning sequence reads, clone sequences and assembly contigs with BWA-MEM. *arXiv:1303.3997 [q-bio]*. Position-wise base counts were performed with IGVtools (21) and resulting wig files were processed to call somatic mutations along the reference sequence with *ad hoc* Python scripts (available on request). Sequences were deposited on the EMBL EBI ENA website, http://www.ebi.ac.uk/ena, under accession number: PRJEB19507.

Statistical analysis

Statistical tests were performed using GraphPad Prism (*$P < 0.05$, **$P < 0.01$, ***$P < 0.001$, ****$P < 0.0001$).

RESULTS

Generation of c3'RR mice

We generated a mouse model with an *IgH* locus carrying a miniaturized 'core-3'RR' (*c3'RR*). Our gene-targeting strategy replaced the entire *3'RR* region (i.e. 30.3 kb) with the *c3'RR* (2.1 kb), which encompassed only the four core enhancers (*hs3a*, *hs1.2*, *hs3a* and *hs4*) (Figure 1A). To optimize gene targeting, we used CRISPR/cas 9 in order to generate double-strand breaks at both ends of the 3'RR and initiate recombination. The targeting vector was co-transfected with CRISPR/cas9 vectors in CK35 ES cells. We obtained three positive clones out of 15 tested. After germline transmission, mice were bred with *cre* expressing mice to delete the Neo^R cassette. In this study, *c3'RR* mice were compared to *Δ3'RR* (10) and *ΔIRIS* mice (14) (Figure 1B).

B-cell development

To study B-cell development in *c3'RR* mice, we generated heterozygous $c3'RR^a/wt^b$ mice by crossing homozygous $c3'RR^a/c3'RR^a$ (IgH^a locus from the SV129 strain) mice with C57BL/6 mice (wt^b/wt^b). This allowed us to study the effect of the mutation by comparison with a *wt* IgH locus in the same mouse and in the conditions of an internal competition between cells expressing either the *wt* 'b' allele or the knocked-out 'a' allotype IgH locus. B-cell

development was barely affected in those B-cells expressing a rearranged *c3'RR* allele, although these IgM^a cells were slightly less abundant than in *wt*^{a}/*wt*^{b} mice (Supplementary Figure S1A). Analysis of *c3'RR*^{a}/*wt*^{b} (*vs* *wt*^{a}/*wt*^{b}) splenic B-cells similarly showed a slightly decreased *a*/*b* ratio among transitional (B220$^+$ AA4.1$^+$), follicular (B220$^+$ CD21^{low} CD23^{high}) and marginal zone (B220$^+$ CD21^{high} CD23^{low}) B-cells expressing either the *a* or *b* allotype. (Supplementary Figure S1B).

3'RR core enhancers are sufficient to induce CSR, but with a partial defect

We explored Ig production *in vitro* and *in vivo* upon extracting 3'RR core enhancers from their packaging DNA. When first examining secreted Ig levels and plasma accumulation *in vivo* (Figure 2A), we observed that Ig classes with short-half-lives and notably IgM and IgA were present at lower levels than in *wt* animals, in contrast with roughly normal amounts of those IgG classes with long half-lives, IgG_1 and IgG_3 (which can accumulate, since they are most efficiently recycled after binding to the FcRn receptor) (22,23). Ig steady state plasma levels indeed integrate the rates of both production and catabolism, the latter being decreased in conditions of lowered Ig production and then notably resulting for IgG_1, in a 3-fold increased half-life (22). It has accordingly been observed, by checking *in vitro* cultures, that in several cases of Ig production defects, that *in vivo* serum levels can be apparently preserved even when an Ig production defect is clearly present (8).

We next quantified Ig levels in conditions more directly reflecting Ig production, in supernatants of B-cells activated *in vitro* by LPS and appropriate cytokines. We compared *c3'RR* homozygous cells with either *wt* or homozygous *Δ3'RR* cells known to carry a strong defect in *in vitro* Ig secretion (6). An intermediate, but significant secretion defect was observed for *c3'RR* cells, affecting all IgG classes except IgG_1, while for IgA and IgM, the trend towards a decrease was not significant (Figure 2B).

To better assess *in vivo* Ig production compared to lymphocyte counts, and the role of the 3'RR palindromic shell during immune activation, we quantified the boost in serum IgM and IgG_1 after SRBC immunization in *wt* compared to homozygous 3'RR mutant mice. In pre-immune mice, normal counts of IgM+ lymphocytes contrasted with less serum IgM at the basal state in *c3'RR* and *Δ3'RR* mice; this difference persisted after SRBC activation (although serum IgM levels then increased in all animals, either *wt*, *c3'RR* or *Δ3'RR)* (Figure 3, top panel). To further evaluate the partial independence of IgG_1 from the *c3'RR* mutation, we measured *in vivo* class-switched IgG1+ lymphocytes, which were normal in *c3'RR* mice at the basal state (Figure 3, bottom panel). The serum IgG1 level was also normal at the basal state, in conditions where accumulation and decreased IgG catabolism are known to occur in mice producing low amounts of IgG (22). By contrast, serum IgG_1 was boosted in animals stimulated by SRBC injection, and then remained at a level significantly lower than in *wt* mice, this dynamic production of Ig being more sensitive to an Ig production defect (Figure 3, bottom panel, right).

Independently of Ig secretion, CSR can be measured more directly *in vitro* by following the change in BCR expression. To determine the impact of 3'RR miniaturization on CSR, we evaluated class switching to the various BCR isotypes after specific *in vitro* stimulation. Homozygous *c3'RR*/*c3'RR* cells were compared with either *wt* or homozygous *Δ3'RR* cells carrying a complete 3'RR deletion. Flow cytometry evaluated surface expression of class-switched isotypes on activated splenic B-cells from *wt*, *c3'RR* and *Δ3'RR* mice. As previously described (6), CSR in control *Δ3'RR* cells stimulated for 4 days, was barely detectable for all classes except for IgG_1 (with some IgG_1-producing cells still detectable). Although milder, a CSR phenotype reminiscent of the latter also appeared in *c3'RR* mice: class-switched IgG3 cells decreased to a level intermediate between that observed in *Δ3'RR* and *wt* mice (Supplementary Figure S2), while IgG1$^+$ cells were not affected. In agreement with cell cytometry, Q-PCR in *c3'RR* cells revealed an intermediate decrease in post-switch transcripts (PST), less significant than for the *Δ3'RR* cells and diversely affecting PST from Cγ2b (down to the same low levels as in *Δ3'RR* B-cells), Cα, and to a lesser extent Cγ3, Cγ2a and Cγ1 PST which tended to be lower but did not show a significantly lower level in these experiments (Figure 4A).

We also explored *in vitro* whether the absence of the 3'RR palindromic shell lowered or delayed CSR. We quantified PST daily during a 5-day stimulation and found a decreased level of PST in *c3'RR* animals for *Cγ1*, *Cγ3*, *Cγ2a*, *Cγ2b* at all time points compared to *wt* mice. (Supplementary Figure S3).

Germline transcription (GLT) of a C_H gene is a known prerequisite for CSR. We evaluated GLT in *in vitro* (LPS ± cytokines) activated splenic B cells from *wt*, *c3'RR* and *Δ3'RR* mice. All GLT were partially affected in *c3'RR* mice compared to *wt* and *3'RR* mice (Figure 4B). Altogether, these results indicated that a core-3'RR made up of naked core enhancers supported CSR at a significantly lower level than the full-length *wt* super-enhancer. Similar to *Δ3'RR* mice, where μ chain transcription is roughly normal in lymphocytes expressing membrane IgM but strongly declines (together with IgM secretion) in plasma cells, secreted-type μ transcripts (encoding secreted IgM) in *c3'RR* mice decreased to a level intermediate between *wt* and *Δ3'RR* mice (Figure 4C).

3'RR packaging DNA is mandatory for optimal SHM

Using high throughput next generation sequencing, we explored SHM downstream of rearranged V(D)J genes in the J_H4 intron as described (24) (using the rearranged *Jκ5* intron as a control) in *wt*, *c3'RR* and *Δ3'RR* mice to determine the mechanistic impact of 3'RR alterations. Germinal center B-cells from Peyer's patches were sorted from *wt*, *c3'RR* and *Δ3'RR* mice and analyzed for SHM. In these settings, normal mutation frequencies in *wt* mice at the *IgH* (J_H4 and *Sμ* regions) and *Igk* loci were respectively 13.27‰, 7.7‰ and 11.8‰. As previously documented (10), *Δ3'RR* mice showed a strong SHM defect at the *IgH* J_H4 (1.48‰) and *Sμ* regions (2‰) (Figure 5A and B, Supplementary Figure S4 for positions of mutations and ATGC tables). Strik-

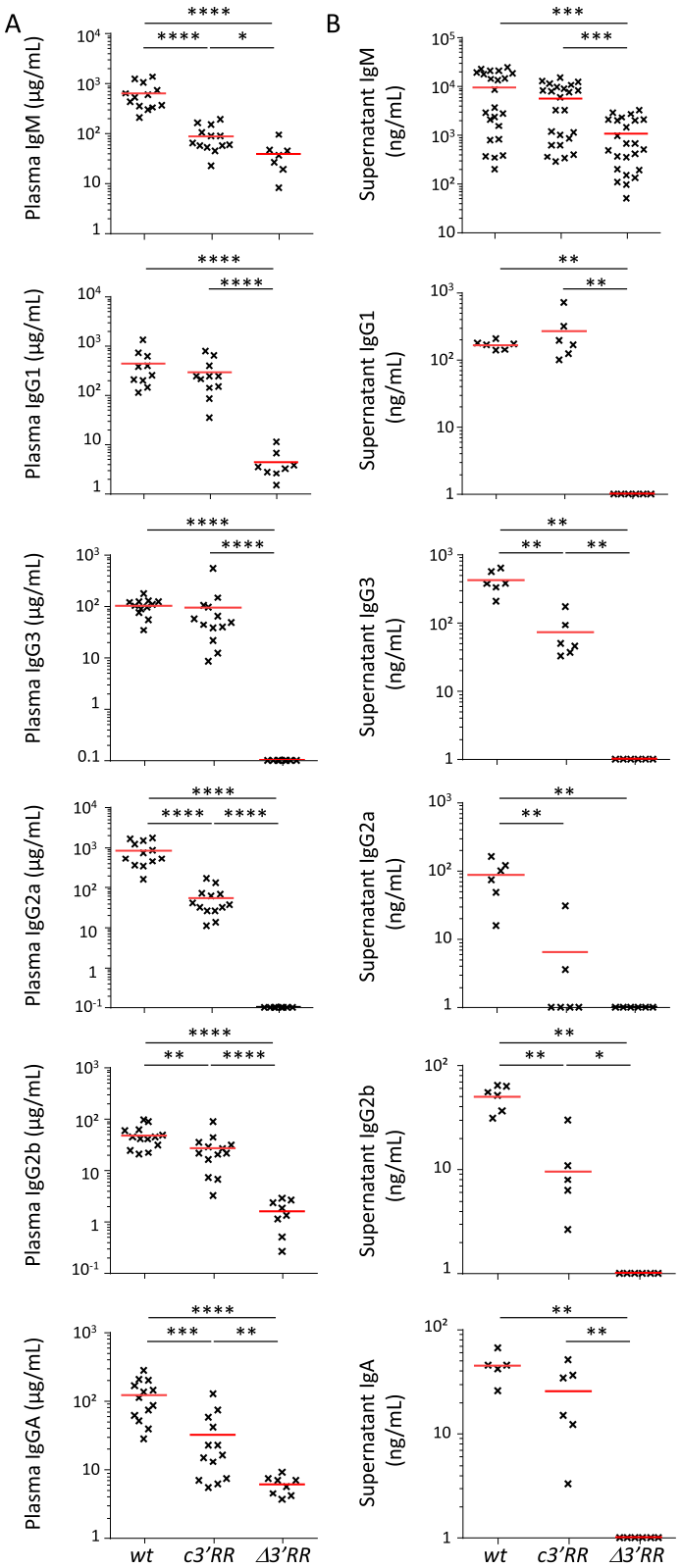

Figure 2. In the absence of packaging DNA, core 3'RR enhancers partially support Ig secretion. (**A**) ELISA analysis of IgM, IgG_1, IgG_{2a}, IgG_{2b}, IgG_3 and IgA in plasma from *Δ3'RR*, *c3'RR* and *wt* mice. (**B**) ELISA analysis of IgM, IgG_1, IgG_{2a}, IgG_{2b}, IgG_3 and IgA in supernatants from LPS ± IL-4, INFγ and TGFβ stimulated splenocytes from *Δ3'RR*, *c3'RR* and *wt* mice. Mean ± SEM of two independent experiments with at least three mice and Mann Whitney test for significance.

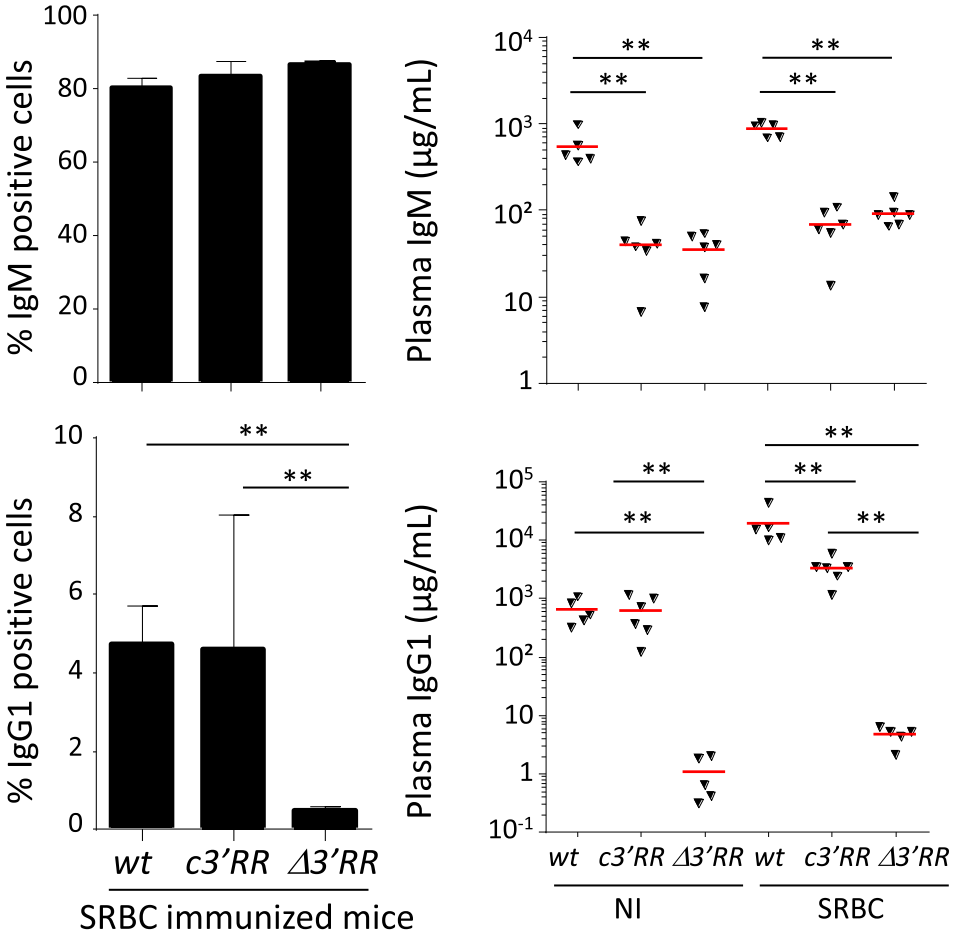

Figure 3. *In vivo* immune stimulation in the absence of 3'RR packaging DNA. FACS analysis of IgM and IgG_1 positive cells at basal state (*left panel*) and ELISA of IgM (*top*) and IgG_1 (*bottom*) in plasma from *Δ3'RR*, *c3'RR* and *wt* mice before (NI) and after SRBC immunization (*right panel*). Mean ± SEM of two independent experiments with three mice each and Mann–Whitney test for significance.

ingly, a similar SHM defect affected *IgH* J_H4 sequences obtained from *c3'RR* mice (1.48‰) indicating that the 3'RR stimulatory effect on *IgH* SHM needs not only core enhancers but also their palindromic packaging DNA. The same analysis was performed in the *Sμ* region, where we again observed a decreased SHM in *c3'RR* mice, at an intermediate level between *wt* and *Δ3'RR* mice (Figure 5A and B).

DISCUSSION

The 3'RR is a strong super-enhancer regulating remodeling of the *IgH* locus in mature B cells and was even recently shown to have *trans*-acting effects on the other IgH allele (1,25). Full deletion of the *3'RR* was previously reported to strongly impact CSR, SHM and the IgH boosted expression which ensures high antibody secretion by plasma cells (6,10). By contrast, this deletion fully preserved early B-cell maturation and marginally impacted membrane IgM density and B-cell fate (toward slightly less marginal zone B-cells) (6,26).

As any super-enhancer, the 3'RR integrates core enhancers buried in packaging DNA. Since transcription factors bind DNAse1 hypersensitive regions of core enhancers, and since large DNA fragments cannot easily be handled, many studies devoted to enhancer function and many transgenes supposedly providing 3'RR models simply omitted this packaging DNA (15–19).

More than 90% of mammalian DNA is non-coding and is often considered as useless (27), while this DNA might in fact play multiple roles, notably architectural. The 3'RR case is very specific due to its unique palindromic structure featuring several kb-long IRISs that flank the central *hs1,2* core enhancer (12,28).

While alterations of the 3'RR made in the endogenous locus were initially shown to affect CSR (7), it was also observed that several precise deletions of a single core enhancer simply had no phenotype, provided the global structure of the 3'RR was maintained and no exogenous gene (such as a *neo* resistance cassette) was left inserted (29–31). By contrast, large deletions affecting multiple enhancers (and more recently a large deletion of the 5′ half of the packaging palindromic DNA), while preserving core enhancers, all severely impacted class switching (8,14). In agreement with these stereotyped CSR alterations following partial knock-outs, deletion of the entire 3'RR resulted in an al-

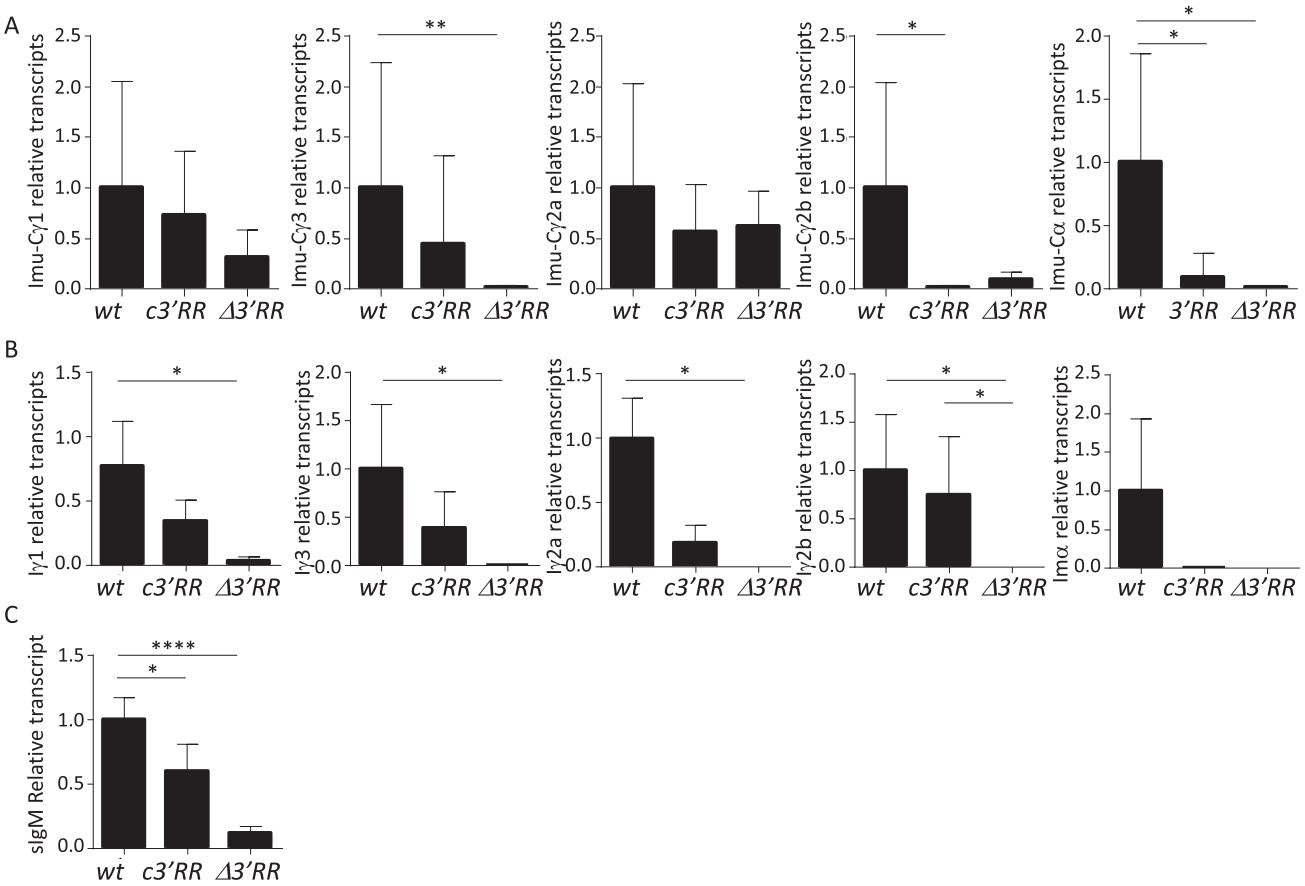

Figure 4. In the absence of packaging DNA, core 3'RR enhancers partially support IgH CSR. (**A**) Post switching transcripts in B splenocytes from *Δ3'RR*, *c3'RR* and *wt* mice. (**B**) Germline transcripts in B splenocytes from *Δ3'RR*, *c3'RR* and *wt* mice. Cells were stimulated with LPS ± IL-4, INFγ and TGFβ for 4 days. $I\gamma_1$-$C_{\gamma 1}$, $I\gamma_{2a}$-$C_{\gamma 2a}$, $I\gamma_{2b}$-$C_{\gamma 2b}$, $I\gamma_3$-$C_{\gamma 3}$ and I_α-C_α GL transcription was evaluated by real-time PCR. (**C**) Bar graphs represent secreted IgM transcripts. Values were normalized to *GAPDH* transcripts. Mean ± SEM of two independent experiments with three mice and Mann–Whitney test for significance.

most complete CSR defect (6). Since miniaturized 3'RR substitutes, linking all four 3'RR core enhancers, have been widely used and considered to provide all 3'RR features, we wished, in the present study, to replace the full-length super-enhancer with its miniaturized (*c3'RR*) counterpart. We then evaluated this replacement in the physiologic context of the endogenous locus. Strikingly, this replacement severely affected CSR to some (IgG_3, IgG_{2a}, IgG_{2b}…) but not all Ig classes (IgG_1 was notably respected). This phenotype was strikingly similar to that of ΔIRIS mice lacking one half of the 3'RR repetitive packaging DNA (14). The *c3'RR* mice also poorly supported SHM and the level of mutation in the rearranged J_H4 intron was in fact similar to that in 3'RR-less B-cells (32). Again, this SHM phenotype was quite similar to that of *ΔIRIS* mice (14).

We finally observed decreased IgH expression in plasma cells indicated by decreased IgM plasma levels in mice and decreased amounts of secreted-type IgM transcripts, at a level intermediate between *wt* and *Δ3'RR* mice, which provided another similarity with the *ΔIRIS* mice (6,14).

Altogether, our data indicate that the DNA shell surrounding core enhancers within the *IgH* 3'RR is not made up of useless junk DNA but, rather, contributes actively to 3'RR function. The ability of 3'RR core enhancers to support CSR and AID recruitment has been demonstrated by several previous studies in transgenes and transfectants and by deletion of the 3'RR *hs3b* and *hs4* core enhancers while respecting most of the 3'RR DNA shell (8,19). The present study shows that while core enhancers are mandatory for full activity of the 3'RR super-enhancer, the surrounding sequences do not constitute useless junk DNA, but instrumentally contribute to 3'RR activity.

These observations clearly deserve to be considered for the future design of transgenic, knock-in or any other mouse engineered for Ig production (notably humanized) if efficient class switching and affinity maturation through SHM is desired.

Regarding the functional anatomy of the 3'RR super-enhancer and given the very strong similarity between the phenotype of *c3'RR* mice and that of *ΔIRIS* mice, our data suggest that the major activity of the 3'RR DNA shell is architectural and related to a necessary large DNA dyad symmetry of the regions flanking *hs1,2*. In that regard, deleting either flank of the palindrome in *ΔIRIS* or the whole palindromic DNA shell in *c3'RR* mice somehow yields a similar phenotype where core enhancers are working on their own and lacking the amplifying effect of the 3'RR 3D-architecture. Inverted repeats might function by posi-

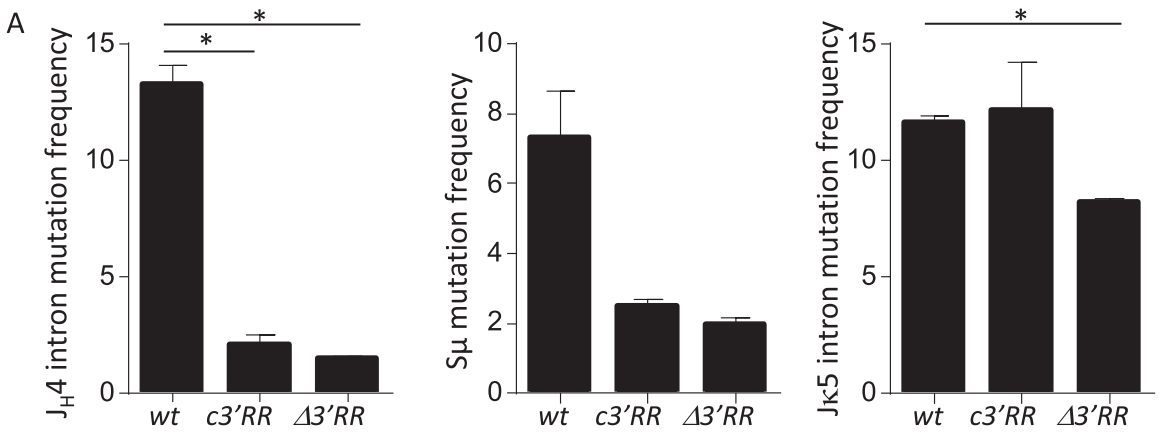

B

	J_H4 intron			Sμ region			Jκ5 intron		
	number (pb)	number of bp analyzed	mutation frequency	number (pb)	number of bp analyzed	mutation frequency	number (pb)	number of bp analyzed	mutation frequency
wt	3 836 055	289 145 399	13.27‰	1 630 636	211 840 812	7.7‰	694 540	58 858 241	11.8‰
c3'RR	559 914	283 135 387	1.98‰	513 593	205 274 215	2.5‰	5 661 206	508 248 496	11.14‰
Δ3'RR	683 201	461 026 844	1.48‰	600 019	297 170 448	2‰	7 617 971	930 031 623	8.19‰

Figure 5. Core 3'RR enhancers do not optimally support SHM. (**A**) Somatic hypermutation at J_H4 intron (*left*), *Sμ* (*middle*) and *Jκ5* intron (*right*) of Peyer's patch GC B-cells sorted from *Δ3'RR*, *c3'RR* and *wt* mice. Data were obtained from two to three mice per group. T-test two-sided with Welch's correction for significance. (**B**) Number of mutations, bp analysed and mutation frequency at J_H4 intron, *Jκ5* intron and *Sμ* region for *Δ3'RR*, *c3'RR* and *wt* mice. Data represent a pool of at least two mice.

tioning the *3'RR* in its optimal 3D-configuration, together with eRNA, lncRNA-CSR and transcription factors in order to stabilize a chromosomal organization that most efficiently recruits AID to mammalian *IgH* loci. Interestingly, we found no inverted repeats similar to those in the 3'RR around the mouse and human intronic *Eμ* or around *Eκ* and the *3'κ* enhancer. We found no palindrome either around the zebrafish *IgH* intronic and 3′ regulatory elements (33). An attractive hypothesis is thus that the peculiar 3'IgH structure found in all mammals has been evolutionarily selected and contributes to the highly efficient class switching and somatic hypermutation that occurs in mammalian B cells.

SUPPLEMENTARY DATA

Supplementary Data are available at NAR Online.

ACKNOWLEDGEMENTS

We acknowledge the technological expertise of E. Guerin from the GENOLIM core facility of the Limoges University (France). We thank S. Desforges and B. Remérand for help with animal care.
Authors contribution: S. Le Noir, M. Brousse and S. Lecardeur actively performed the experimental part of the study. M. Cogné and S. Le Noir designed and supervised the project. Z. Oruc helped generating transgenic mice. F. Boyer performed the bio informatics analysis. Le Noir S., Cogné M., Denizot Y. and Cook-Moreau J. participated in the scientific discussion for manuscript writing.

FUNDING

Institut Universitaire de France and Association pour la Recherche sur le Cancer (to S.L.N.); ALURAD and Fondation partenariale de l'Université de Limoges (to F.B.); ARC [PGA120150202338]; Agence Nationale de la Recherche [ANR grants 16-CE15-0019-01 and EpiSwitch-3'RR 2016]; Institut National du Cancer [INCA9363, FOHLY2 2013-085]; Ligue Nationale contre le Cancer and Région Aquitaine-Limousin-Poitou-Charente. Funding for open access charge: Limoges University.
Conflict of interest statement. None declared.

REFERENCES

1. Pinaud,E., Marquet,M., Fiancette,R., Péron,S., Vincent-Fabert,C., Denizot,Y. and Cogné,M. (2011) The IgH locus 3′ regulatory region: pulling the strings from behind. *Adv. Immunol.*, **110**, 27–70.
2. Whyte,WA., Orlando,DA., Hnisz,D., Abraham,BJ., Lin,CY., Kagey,MH., Rahl,P.B., Lee,T.I. and Young,R.A. (2013) Master transcription factors and mediator establish super-enhancers at key cell identity genes. *Cell*, **153**, 307–319.
3. Pefanis,E., Wang,J., Rothschild,G., Lim,J., Kazadi,D., Sun,J., Federation,A., Chao,J., Elliott,O., Liu,Z.P. *et al.* (2015) RNA exosome-regulated long non-coding RNA transcription controls super-enhancer activity. *Cell*, **161**, 774–789.
4. Rouaud,P., Vincent-Fabert,C., Fiancette,R., Cogné,M., Pinaud,E. and Denizot,Y. (2012) Enhancers located in heavy chain regulatory region (hs3a, hs1,2, hs3b, and hs4) are dispensable for diversity of VDJ recombination. *J. Biol. Chem.*, **287**, 8356–8360.
5. Braikia,F.-Z., Conte,C., Moutahir,M., Denizot,Y., Cogné,M. and Khamlichi,A.A. (2015) Developmental switch in the transcriptional activity of a long-range regulatory element. *Mol. Cell. Biol.*, **35**, 3370–3380.
6. Vincent-Fabert,C., Fiancette,R., Pinaud,E., Truffinet,V., Cogné,N., Cogné,M. and Denizot,Y. (2010) Genomic deletion of the whole IgH

3′ regulatory region (hs3a, hs1,2, hs3b, and hs4) dramatically affects class switch recombination and Ig secretion to all isotypes. *Blood*, **116**, 1895–1898.
7. Cogné,M., Lansford,R., Bottaro,A., Zhang,J., Gorman,J., Young,F., Cheng,H.L. and Alt,F.W. (1994) A class switch control region at the 3′ end of the immunoglobulin heavy chain locus. *Cell*, **77**, 737–747.
8. Pinaud,E., Khamlichi,AA., Le Morvan,C., Drouet,M., Nalesso,V., Le Bert,M. and Cogné,M. (2001) Localization of the 3′ IgH locus elements that effect long-distance regulation of class switch recombination. *Immunity*, **15**, 187–199.
9. Péron,S., Laffleur,B., Denis-Lagache,N., Cook-Moreau,J., Tinguely,A., Delpy,L., Denizot,Y., Pinaud,E. and Cogné,M. (2012) AID-driven deletion causes immunoglobulin heavy chain locus suicide recombination in B cells. *Science*, **336**, 931–934.
10. Rouaud,P., Vincent-Fabert,C., Saintamand,A., Fiancette,R., Marquet,M., Robert,I., Reina-San-Martin,B., Pinaud,E., Cogné,M. and Denizot,Y. (2013) The IgH 3′ regulatory region controls somatic hypermutation in germinal center B cells. *J. Exp. Med.*, **210**, 1501–1507.
11. Bonaud,A., Lechouane,F., Le Noir,S., Monestier,O., Cogné,M. and Sirac,C. (2015) Efficient AID targeting of switch regions is not sufficient for optimal class switch recombination. *Nat. Commun.*, **6**, 7613.
12. Chauveau,C. and Cogné,M. (1996) Palindromic structure of the IgH 3′ locus control region. *Nat. Genet.*, **14**, 15–16.
13. Chauveau,C., Pinaud,E. and Cogne,M. (1998) Synergies between regulatory elements of the immunoglobulin heavy chain locus and its palindromic 3′ locus control region. *Eur. J. Immunol.*, **28**, 3048–3056.
14. Saintamand,A., Vincent-Fabert,C., Garot,A., Rouaud,P., Oruc,Z., Magnone,V., Cogné,M. and Denizot,Y. (2016) Deciphering the importance of the palindromic architecture of the immunoglobulin heavy-chain 3′ regulatory region. *Nat. Commun.*, **7**, 10730.
15. Madisen,L. and Groudine,M. (1994) Identification of a locus control region in the immunoglobulin heavy-chain locus that deregulates c-myc expression in plasmacytoma and Burkitt's lymphoma cells. *Genes Dev.*, **8**, 2212–2226.
16. Wang,J. and Boxer,L.M. (2005) Regulatory elements in the immunoglobulin heavy chain gene 3′-enhancers induce c-myc deregulation and lymphomagenesis in murine B cells. *J. Biol. Chem.*, **280**, 12766–12773.
17. Truffinet,V., Pinaud,E., Cogné,N., Petit,B., Guglielmi,L., Cogné,M. and Denizot,Y. (2007) The 3′ IgH locus control region is sufficient to deregulate a c-myc transgene and promote mature B cell malignancies with a predominant Burkitt-like phenotype. *J. Immunol.*, **179**, 6033–6042.
18. Xiang,H., Noonan,EJ., Wang,J., Duan,H., Ma,L., Michie,S. and Boxer,L.M. (2011) The immunoglobulin heavy chain gene 3′ enhancers induce Bcl2 deregulation and lymphomagenesis in murine B cells. *Leukemia*, **25**, 1484–1493.
19. Dunnick,W.A., Shi,J., Fontaine,C. and Collins,J.T. (2013) Transgenes of the mouse immunoglobulin heavy chain locus, lacking distal elements in the 3′ regulatory region, are impaired for class switch recombination. *PLoS ONE*, **8**, e55842.
20. Kim,A., Han,L., Santiago,G.E., Verdun,R.E. and Yu,K. (2016) Class-switch recombination in the absence of the IgH 3′ regulatory region. *J. Immunol.*, **197**, 2930–2935.
21. Robinson,JT., Thorvaldsdóttir,H., Winckler,W., Guttman,M., Lander,ES., Getz,G. and Mesirov,J.P. (2011) Integrative genomics viewer. *Nat. Biotechnol.*, **29**, 24–26.
22. Fahey,J.L. and Sell,S. (1965) The immunoglobulins of mice. V. The metabolic (catabolic) properties of five immunoglobulin classes. *J. Exp. Med.*, **122**, 41–58.
23. Akilesh,S., Christianson,G.J., Roopenian,D.C. and Shaw,A.S. (2007) Neonatal FcR expression in bone marrow-derived cells functions to protect serum IgG from catabolism. *J. Immunol.*, **179**, 4580–4588.
24. Jolly,C.J., Klix,N. and Neuberger,M.S. (1997) Rapid methods for the analysis of immunoglobulin gene hypermutation: application to transgenic and gene targeted mice. *Nucleic Acids Res.*, **25**, 1913–1919.
25. Le Noir,S., Laffleur,B., Carrion,C., Garot,A., Lecardeur,S., Pinaud,E., Denizot,Y., Skok,J. and Cogné,M. (2017) The IgH locus 3′ cis-regulatory super-enhancer co-opts AID for allelic transvection. *Oncotarget.*, **8**, 12929–12940.
26. Saintamand,A., Rouaud,P., Garot,A., Saad,F., Carrion,C., Oblet,C., Cogné,M., Pinaud,E. and Denizot,Y. (2015) The IgH 3′ regulatory region governs μ chain transcription in mature B lymphocytes and the B cell fate. *Oncotarget.*, **6**, 4845–4852.
27. Palazzo,A.F. and Gregory,T.R. (2014) The case for junk DNA. *PLoS Genet.*, **10**, e1004351.
28. D'Addabbo,P., Scascitelli,M., Giambra,V., Rocchi,M. and Frezza,D. (2011) Position and sequence conservation in amniota of polymorphic enhancer HS1.2 within the palindrome of IgH 3′ regulatory region. *BMC Evol. Biol.*, **11**, 71.
29. Manis,JP., van der Stoep,N., Tian,M., Ferrini,R., Davidson,L., Bottaro,A. and Alt,F.W. (1998) Class switching in B cells lacking 3′ immunoglobulin heavy chain enhancers. *J. Exp. Med.*, **188**, 1421–1431.
30. Vincent-Fabert,C., Truffinet,V., Fiancette,R., Cogné,N., Cogné,M. and Denizot,Y. (2009) Ig synthesis and class switching do not require the presence of the hs4 enhancer in the 3′ IgH regulatory region. *J. Immunol.*, **182**, 6926–6932.
31. Bébin,A-G., Carrion,C., Marquet,M., Cogné,N., Lecardeur,S., Cogné,M. and Pinaud,E. (2010) In vivo redundant function of the 3′ IgH regulatory element HS3b in the mouse. *J. Immunol.*, **184**, 3710–3717.
32. Rouaud,P., Vincent-Fabert,C., Saintamand,A., Fiancette,R., Marquet,M., Robert,I., Reina-San-Martin,B., Pinaud,E., Cogné,M. and Denizot,Y. (2013) The IgH 3′ regulatory region controls somatic hypermutation in germinal center B cells. *J. Exp. Med.*, **210**, 1501–1507.
33. Danilova,N., Saunders,H.L., Ellestad,K.K. and Magor,B.G. (2011) The zebrafish IgH locus contains multiple transcriptional regulatory regions. *Dev. Comp. Immunol.*, **35**, 352–359.